

Investigation the connection between the intermediate gamma-ray bursts and X-ray flashes

József Kóbori¹, Zsolt Bagoly¹, Lajos G. Balázs^{2,3} and István Horváth⁴

¹Dept. of Physics of Complex Systems, Eötvös University, Budapest, Hungary, jkobori@caesar.elte.hu

²MTA CSFK Konkoly Observatory, Budapest, Hungary,

³Dept. of Astronomy, Eötvös University, Budapest, Hungary,

⁴Dept. of Physics, National University of Public Service, Budapest, Hungary

Abstract

Gamma-ray bursts (GRBs) can be divided into three groups: short-, intermediate- and long-duration bursts. While the progenitors of the short and long ones are relatively known, the progenitor objects of the intermediate-duration bursts (IBs) are generally unknown, however, recent statistical studies suggest, that they can be related to the long-duration bursts. Another types of GRBs are the so-called X-ray flashes (XRFs) and X-ray rich GRBs (XRRs). The former ones radiate more intensively in the X-ray bands than common GRBs, but in the cases of XRFs the main component of the emission is produced entirely at X-ray wavelengths. Also, the XRFs and IBs show some similarities regarding their prompt- and afterglow properties. In this work we investigate whether there is a difference between the global parameters of the X-ray flashes and intermediate-duration group of gamma-ray bursts. The statistical tests do not show any significant discrepancy regarding most of the parameters, except the BAT photon index, which is only a consequence of the definition of the XRFs.

1 Introduction

Gamma-ray bursts are a mysterious phenomenon since their discovery in 1967. In 1993, Kouveliotou et al. (1993), based on statistical studies showed that two types of GRBs can be distinguished using the T_{90} quantity (T_{90} is the time during which the cumulative counts increase from 5% to 95% above the background, thus encompassing 90% of the total GRB counts): the short- ($T_{90} < 2$ s) and long-duration ($T_{90} > 2$ s) bursts. Later on, Horváth (1998) and Mukherjee et al. (1998) in 1998 independently have found, that an intermediate-duration type of bursts exists as well. These bursts can be connected to the short- (e.g. Řípa et al. 2012) and long-duration (e.g. Veres et al. 2010) bursts as well depending on the particular gamma-ray satellite used for constructing the sample. Since then some other types of bursts were identified: X-ray rich bursts and X-ray flashes. Statistical analyses suggest (e.g. Sakamoto et al. 2008) that common-GRBs, XRRs and XRFs can be drawn from the same population. However, the debate about the underlying physics is still going on, but thanks to the *Swift* mission (Gehrels et al. 2004), studying the simultaneous observations at many wavelengths allow us to constrain some of the prompt- and afterglow-emission parameters for the various types of bursts.

In this paper we report a statistical study of the prompt and afterglow emission of the intermediate group of GRBs and X-ray flashes. In §2 we describe the classification method of GRBs, then, in §3 we investigate the global parameters of the BAT lightcurves and spectra. After that, in §4 the XRT properties are analysed, while UVOT afterglows are presented in §5.

2 The data sample and the classification method

The sample used in this paper was created by Veres et al. (2010), who classified the bursts using the model based clustering (Bayesian Information Criterion) method. This method gives a probability that a burst belongs to a group, instead of a definite membership. For details of the process, please see their article. The sample consists of 408 bursts up to GRB090726: 331 long, 46 intermediate and 31 short bursts. All of the bursts were detected by the *Swift* satellite. The observational data was downloaded from the *Swift* Science Data Center (BAT fluence, XRT 11- and 24-hour flux, XRT Column Density (NH), BAT 1-sec peak photon flux, BAT photon index, XRT spectral index) and The *Swift*-XRT GRB Catalogue (temporal decay indices, break times).

Among the 46 intermediate bursts there are 38 bursts for which temporal decay indices are available in the XRT Catalogue, but further 5 bursts are excluded, because their lightcurve consists of more than 2 breaks and one or more flares (in these cases because of the flare activity it is difficult to fit the lightcurve, hence determine the underlying afterglow decay index). So, in the following calculations we analysed 33 bursts, and on the figures below 33 bursts are plotted as well.

If we apply the definition for XRFs adopted by Sakamoto et al. (2008) ($H_{32} < 0.76$, where H_{ij} (i, j mark two energy intervals) is the ratio of the fluences in different channels for a given burst using the usual *Swift* energy bands with 10 – 25 – 50 – 100 – 150 keV as their boundaries, so $H_{32} = \frac{S_{50-100}}{S_{25-50}}$), then we can find 20 XRFs and 13 IBs in our sample.

To test whether the XRFs and IBs are drawn from the same population we compared their emission properties applying the Kolmogorov-Smirnov test to the data.

3 BAT fluences, peak fluxes and photon indices

A thorough analysis of the *Swift* BAT (γ -detector) and XRT (X-ray detector) data was carried out by Sakamoto et al. (2008), who investigated the spectral and temporal characteristics of the prompt- and X-ray afterglow-emission of XRFs and XRRs detected by *Swift* between 2004 December and 2006 September. They have found that XRFs, XRRs and the common GRBs form a single broad distribution. For

comparison, we constructed (Fig. 2) the histogram of the quantity $(H_{32})^{-1}$ of our sample for the long-duration bursts, and it confirms the previous result (common distribution for ordinary GRBs, XRFs and XRRs). Nevertheless, if we plot the H_{32} against the T_{90} for the entire sample (short, intermediate and long GRBs) (1) we can see that the boundary for XRFs overlap the range of IBs.

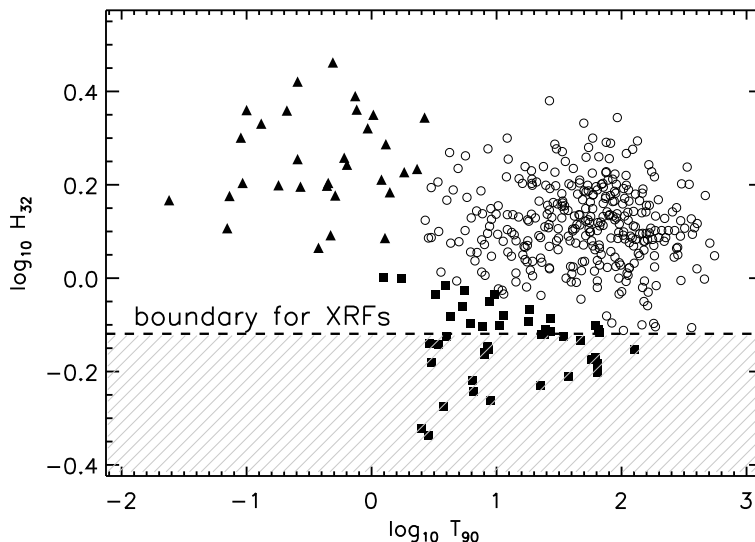


Figure 1: On the figure we plotted the entire sample consisting the long (open circles), intermediate (filled squares) and short GRBs (filled triangles). The dashed line marks the boundary for XRFs defined by Sakamoto et al. (2010), that is, if $H_{32} < 0.76$ the burst is identified as an X-ray flash.

This result is discussed in details by Veres et al. (2010), and it suggests a connection between XRFs and IBs. If we take a look at the histogram of BAT fluences measured between 15-150 keV (Fig. 3), we can see that there is no difference in the distribution of XRF's and IB's BAT fluences. The KS test supports this hypothesis with significance of 0.87. In the cases of the BAT 1-sec peak photon fluxes (Fig. 4), the result is similar, the null hypothesis is accepted with significance of 0.28.

Contrary to the similarities in the fluence and peak flux distributions, a remarkable discrepancy can be observed in the distribution of the BAT photon indices. The reason of this bias is that the constrain for the XRFs ($H_{32} < 0.76$) was defined arbitrarily, which means, that if we choose a higher value for H_{32} as the boundary, then the difference in the distribution simply disappears.

4 XRT temporal and spectral indices

We also compared the distributions of XRT afterglow properties of the XRFs and IBs.

On Fig. (6) we plotted the initial temporal indices, which characterise the first power-law segment of the XRT afterglows. In the distribution of the first break time (Fig. 7) a slight difference can be discovered, the X-ray flashes tend to have this break earlier than the intermediate bursts.

Investigating the α_1 and α_2 indices ($F \propto t^{-\alpha_i}$), the similarity between the XRFs and IBs still holds on, the significances for being drawn from the same populations are 0.42 and 0.35, respectively. The KS test also accepts the same population hypothesis for the XRT fluxes measured at 11 and 24 hours after

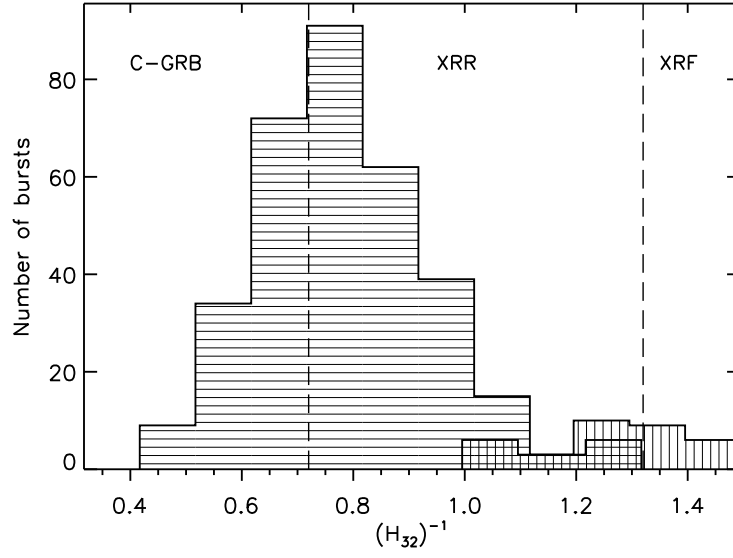


Figure 2: Distributions of the fluence ratio $S(25-50 \text{ keV})/S(50-100 \text{ keV})$ in our sample for long bursts (horizontal line area) and intermediate bursts (vertical line area). The dashed lines correspond to the borders between common-GRBs and XRRs, and between XRRs and XRFs.

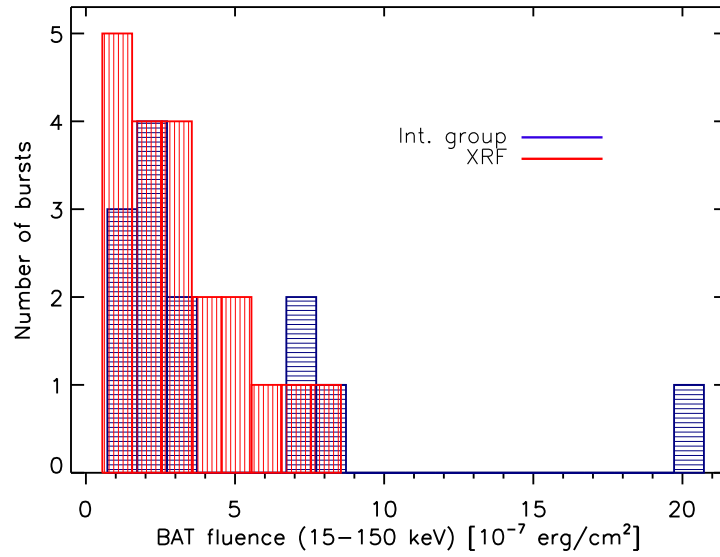


Figure 3: The histogram shows the distribution of the BAT fluences for XRFs and IBs. As it can be clearly observed, the XRFs and IBs form a unique population regarding the BAT fluence.

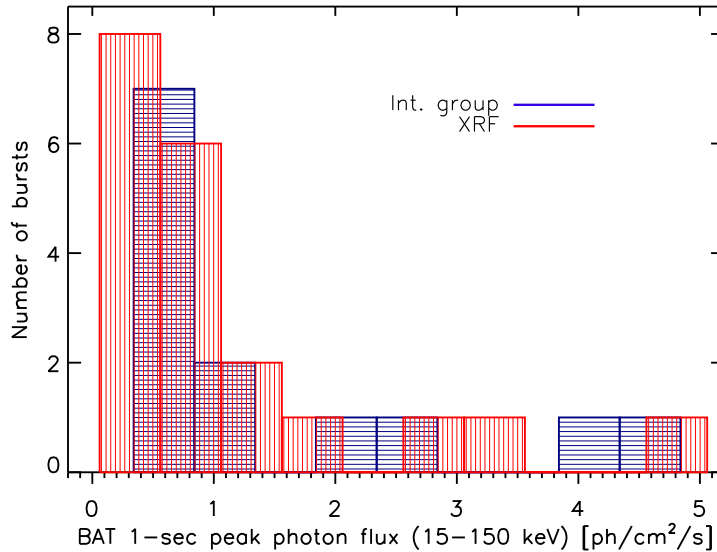


Figure 4: On the figure the distribution of the BAT 1-sec peak photon fluxes can be seen. The KS test indicates that the different types of bursts are drawn from the same population.

the trigger with probabilities of 28% and 11%, which is not surprising, since the α_1, α_2 indices form the same distribution as well. The distributions of the neutral hydrogen column densities (Fig. 9) in the host galaxies calculated from the XRT afterglows indicate that the XRFs and IBs tend to occur in similar type of galaxies, this is confirmed by the KS test, the same population hypothesis has significance of 0.43.

Finally, we constructed the XRT lightcurves of the XRFs and IBs (Fig. 10). As the distribution of the initial temporal decay indices suggests (Fig. 6), the XRF afterglows have a steeper initial phase, but after the first break the decay rates are consistent between the two groups.

5 UVOT afterglows

From the 46 IB, 15 has UVOT observations, but only 11 of them is bright enough to construct the optical lightcurve. After applying the criterion for XRFs, it turns out, that from the 11 afterglows 4 belong to the IBs and 7 belong to the XRFs.

Regarding the optical lightcurves there is not any difference between the lightcurves of XRFs and IBs, they lie in the same flux range (Fig. 11).

6 Conclusion

Veres et al. (2010), based on the H_{32} and T_{90} distributions, showed that the IBs and XRFs probably have the same physical origin, the observable differences in the γ -, X-ray and optical bands may be the consequences of the minor changes in the underlying physical processes, circumburst medium properties and/or observational effects. Our main result in this article that beside the above mentioned T_{90} and H_{32} the IBs and XRFs show similar properties regarding the other observed (γ -, X-ray and optical) quantities

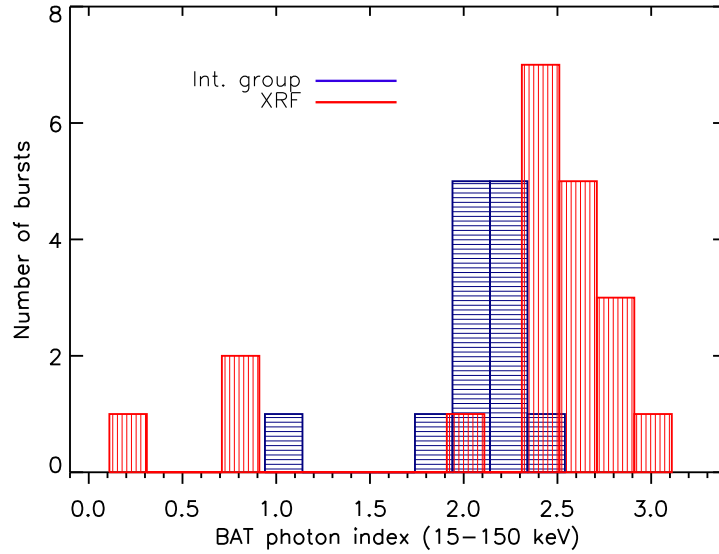


Figure 5: If we examine the distribution of the BAT photon index, a marginal distinction can be revealed between the XRFs and IBs, but it is not surprising, since the boundary for the XRFs ($H_{32} < 0.76$) was defined arbitrarily. If we set this value higher, the significance of the discrepancy becomes lower and finally disappears.

detected by the *Swift* gamma-ray satellite. We have to emphasize that our conclusion concerns GRBs observed *only* by the *Swift*.

Acknowledgements

This research has made use of data obtained through the High Energy Astrophysics Science Archive Research Center Online Service, provided by the NASA/Goddard Space Flight Center and the data supplied by the UK Swift Science Data Centre at the University of Leicester. This study was supported by the Hungarian OTKA grant No. T77795.

References

- [1] Gehrels, N., Chincarini, G., Giommi, P., et al.: 2004, *ApJ* 611, 1005
- [2] Horváth, I.: 1998, *ApJ* 508, 757
- [3] Kouveliotou, C., Meegan, C. A., Fishman, G. J., Bhat, N. P., Briggs, M. S., Koshut, T. M., Paciesas, W. S., Pendleton, G. N., et al.: 1993, *ApJ* 413, L101
- [4] Mukherjee, S., Feigelson, E. D., Babu, G. J., Murtagh, F., Fraley, C., Raftery, A.: 1998, *ApJ* 508, 314
- [5] Sakamoto, T., Hullinger, D., Sato, G., et al.: 2008, *ApJ* 679, 570
- [6] Řípa, j., Mészáros, A., Veres, P., Park, I. H.: 2012, *ApJ* 756, 44
- [7] Veres, P., Bagoly, Z., Horváth, I., Mészáros, A., Balázs, L. G.: 2010, *ApJ* 725, 1955

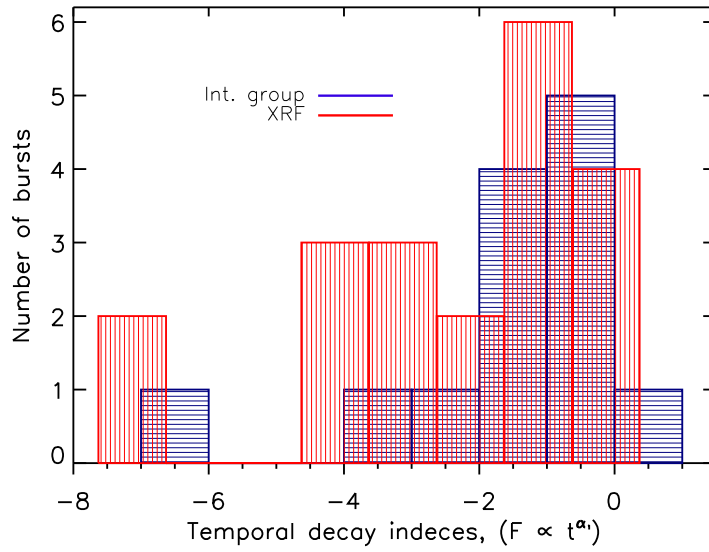


Figure 6: The initial (α_1) XRT decay indices are similar for the XRFs and IBs. The KS test does not suggest any difference between the distributions (the significance for having the same parent distribution hypothesis is 0.35).

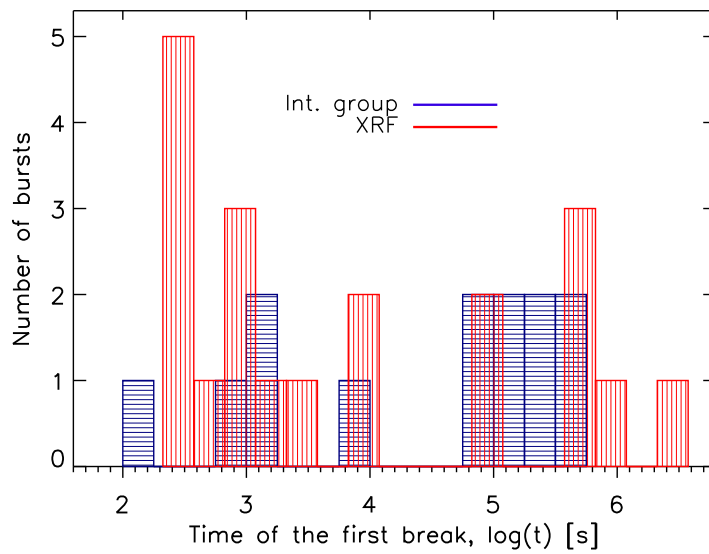


Figure 7: The figure clearly shows, that the first break in the XRT lightcurves appears to happen earlier for the majority of the XRFs, although, the KS test gives a probability only of 89% for having different populations.

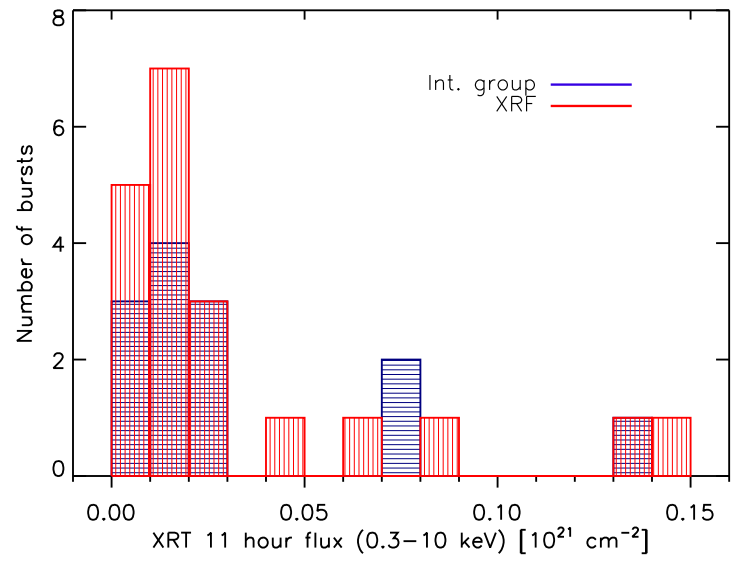


Figure 8: The distribution of the XRT fluxes measured at 11 hours after the trigger confirms the previous results.

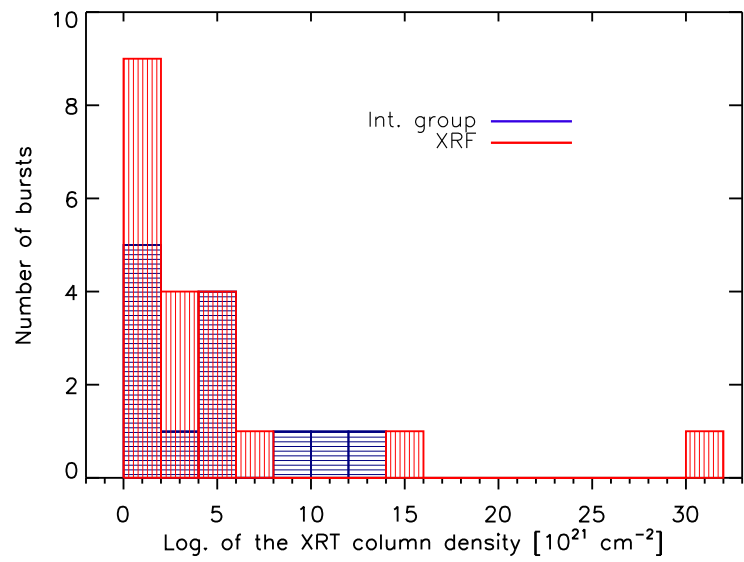


Figure 9: As the majority of other prompt and afterglow parameters, the neutral hydrogen column densities of XRFs and IBs form a single population.

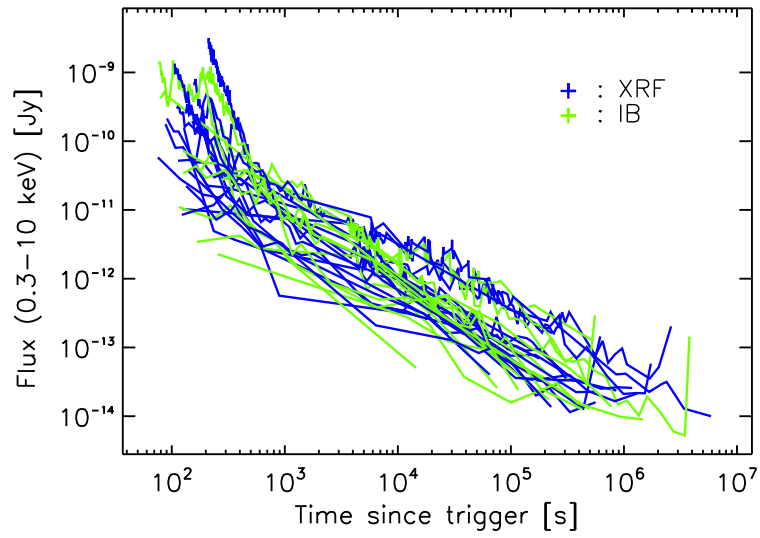


Figure 10: As it can be observed, most of the XRFs have a lightcurve with steeper initial temporal phase, but after the first break, there is no difference in the decay index distribution.

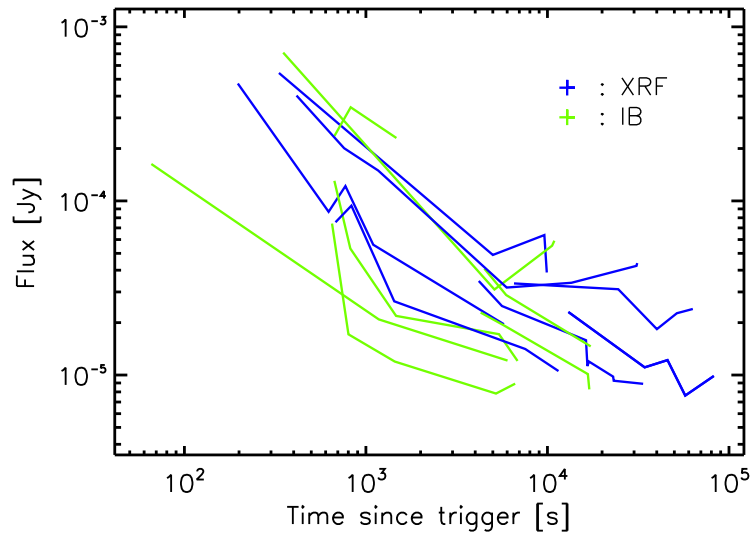


Figure 11: On the figure the UVOT (V, B and U) lightcurves of XRFs and IBs can be observed. The figure does not suggest any discrepancy among the XRFs and IBs.